ACS SENSORS

pubs.acs.org/acssensors

Article

AuNP-Amplified Surface Acoustic Wave Sensor for the Quantification of Exosomes

Chenyun Wang,[†] Cancan Wang,[†] Dan Jin, Yi Yu, Fan Yang, Yulin Zhang, Qunfeng Yao, and Guo-Jun Zhang*

Cite This: *ACS Sens.* 2020, 5, 362−369

Read Online

ACCESS | Metrics & More | Article Recommendations | Supporting Information

ABSTRACT: In this study, we report a gold nanoparticle (AuNP)-amplified surface acoustic wave (SAW) sensor for exosome detection with high sensitivity. The SAW chip was self-assembled with mercapto acetic acid to generate carboxylic groups via the Au−S bond. Anti-CD63 was then anchored onto the chip by pretreatment with 1-(3-dimethylaminopropyl)-3-ethylcarbodiimide hydrochloride (EDC) and *N*-hydroxysuccinimide,1-hydroxypyrrolidine-2,5-dione (NHS). Due to the existence of a membrane protein, CD63, on the exosome surface, exosomes could be bound onto the antibody-immobilized SAW chip. To amplify the detection signal, both the biotin-conjugated epithelial cell adhesion molecule (EpCAM) antibody as a secondary antibody and AuNP-labeled streptavidin were applied onto the exosome-bound SAW chip, resulting in AuNP assembly on the chip through biotin−avidin recognition. The sensor was capable of detecting 1.1×10^3 particles/mL exosomes, which was about 2 orders of magnitude higher than those detected by the strategy without using signal amplification. The sensor also achieved a satisfactory specificity and could detect the low-abundance exosomes directly in blood samples from cancer patients with minimal disturbance. This makes the SAW sensor useful for early diagnosis of cancer.

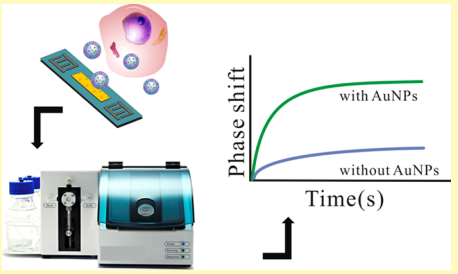

KEYWORDS: *surface acoustic wave, biosensor, exosome, detection, gold nanoparticles, signal amplification*

INTRODUCTION

Early diagnosis of cancer is the most effective way to conquer cancer.[1] Tissue biopsy remains the gold standard for the diagnosis of cancer, but there are many limitations, such as its invasiveness and failing to reflect tumor spatial heterogeneity.[2−4] Liquid biopsy, as a minimally invasive and low-cost method, has a promising future to diagnose different types of cancer by identifying congenital and acquired aberrations that are closely related to cancer occurrence and development.[5,6]

Exosomes (30−150 nm), as the subtype of extracellular vesicles (EVs), are bilayer membrane vesicles secreted by a variety of mammalian cells.[6−9] Exosomes have been confirmed to exist in a wide range of body fluids including serum, urine, breast milk, saliva malignant pleural effusions, bronchial lavage fluid, tears, nasal lavage fluid, semen, synovial fluid, amniotic fluid, etc.[10−12] While circulating in biofluids, exosomes serve as important mediators of intercellular communication that has a close relationship with the development and progression of diseases.[10,13−15] Exosomes have now been widely considered as new-generation biomarkers because of their superiority over other liquid biopsy sources in many respects: more homogeneous in size, higher content in biofluids, more specific markers (RNAs, DNAs, lipids, and proteins), etc.[14,16]

Exosome analysis has enormously drawn interests over the past few years. Transmission electron microscopy (TEM) can offer high-resolution images of exosomes, but it requires extensive sample fixation.[17] Cryoelectron microscopy can determine the original state of exosomes, but it needs high operation technology.[18] Atomic force microscopy (AFM) can offer information about the surface topography, local stiffness, and adhesion properties of exosomes.[19,20] Dynamic light scattering (DLS) can determine the effective particle size of exosomes in biofluids.[21] Nanoparticle tracking analysis (NTA) can provide information about the concentration and size distribution of exosomes.[22] Tunable resistive pulse sensing (TRPS) can also be widely used to measure the concentration and size distribution of exosomes.[23,24] The above-mentioned methods are, however, all about the physical characterization of exosomes.[25] Western blotting and enzyme-linked immunosorbent assay (ELISA) have the ability to quantify the targeted membrane proteins of exosomes.[26] Mass spectrometry enables to identify, quantify, and validate proteins in exosomes. Flow cytometry is capable of characterizing the membrane proteins of exosomes by binding micron-sized latex beads and stained fluorescent antibodies, respectively.[26] A new surface plasma resonance (SPR) platform named a nanoplasmonic exosome (nPLEX) sensor has been used to assay membrane proteins of exosomes.[27] Although many analytical methods exist, the assay

Received: September 24, 2019
Accepted: January 14, 2020
Published: January 14, 2020

https://dx.doi.org/10.1021/acssensors.9b01869
ACS Sens. 2020, 5, 362−369

of exosomes is still a significant challenge due to their ultrasmall size and diversity.[20]

Piezoelectric sensors have attracted enormous interest in the bioassay for their label-free detection, easy operation, and real-time measurement.[28,29] A surface acoustic wave (SAW) sensor holds high sensitivity due to its high operation frequency, which is the commonly employed piezoelectric sensor in the past decades.[30] The measurement principle of the sensor is based on the propagation of surface acoustic waves. Surface acoustic wave sensors are used to detect the quality of the surface load of the sensor chip as well as other fluid properties such as viscoelasticity.[30] When the surface acoustic wave passes through the surface of the chip, its phase changes with the surface quality of the chip.[28] This change can be detected by the instrument and transmitted to a computer via electrical signals. Recently, Li and colleagues reported developing a SAW sensor for the highly sensitive and accurate detection of carcinoembryonic antigen.[31] Zhang et al. described a lithium tantalite ($LiTaO_3$) SAW sensor to investigate the influenza virus in real samples.[32] Chang et al. developed a leaky surface acoustic wave (LSAW) aptasensor with label-free and high-sensitive sensing technology for tumor cell recognition and detection.[33] Our research group also used the SAW sensor to conduct a series of studies. Zhang et al. reported a template-free and surface-confined DNA extension assay based on in situ AgNP growth at the SAW sensor interface to achieve the sequence-specific detection of nucleic acids.[30] Liu and colleagues proposed a graphene-oxide-modified SAW platform based on a single-shot analytical strategy for the label-free detection of CYP2D6*10 gene mutation.[34] Nevertheless, no research works have yet been reported on exosome detection by the SAW sensor.

In this paper, we present the first case of utilizing a SAW biosensor to detect exosomes by employing gold nanoparticle (AuNP) as a signal amplification strategy, as illustrated in Figure 1. The CD63 protein is a member of the trans-membrane-4 superfamily, which is richly found on the surface of exosomes. It has been accepted as the general "exosome" marker, and its expression is not dependent on the phenotype and the origin of the cell. Kanwar and teammates constructed a CD63-modified microfluidic chip to distinguish cancer patients from healthy patients, and the results indicate that the expression level of exosomes in the serum from cancer patients is higher than that from healthy patients.[35] Zhou et al. used an electrochemical method for the identification of exosomes by employing a specific aptamer to recognize CD63 markers on the exosome surface.[36] In view of the specific protein (CD63) on the membrane surface of exosomes, CD63 antibody is modified on the sensor surface and exosomes are bound to the anti-CD63-modified SAW chip via binding between CD63, a membrane protein of the exosomes, and anti-CD63. After that, biotin-labeled EpCAM antibody is specifically bound with exosomes through an epithelial cell adhesion molecule (EpCAM), a cancer-associated antigen whose expression is abundant among the exosomes collected from cancer patients.[37] Since many copies of the markers are exposed on the surface of each exosome, this procedure enables the caputre of efficient exosomes.

To amplify the detection signal, significant changes in the phase shift are observed after streptavidin-labeled AuNP is bound onto the SAW chip via biotin−avidin recognition. Sreptavidin-labeled AuNP is often used to amplify weak signals on the chip surface by increasing the quality of the chip surface. Yao et al. constructed a surface plasmon resonance platform combined with oligonucleotide-capped AuNP to determinate the subattomole oligonucleotides and p53 cDNA.[38] Wang and colleagues proposed surface plasmon resonance with dual AuNP-assisted signal amplification to achieve the direct quantification of cancerous exosomes.[39] With the signal amplification effect produced by AuNP, this established SAW biosensor offers a bioassay platform for the basic research and clinical application of exosomes.

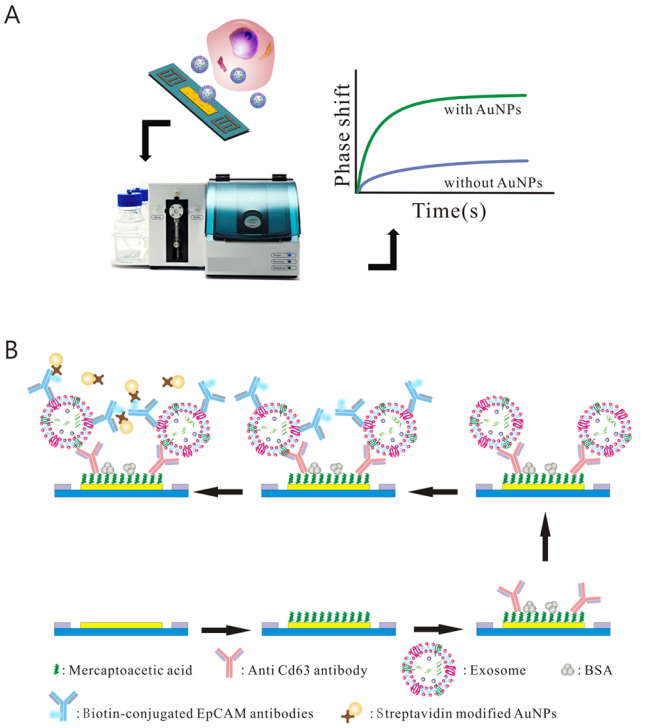

Figure 1. (A) Schematic illustration of a signal-amplified SAW biosensor for highly specific and sensitive detection of exosomes. (B) Modification process of the SAW chip by a double antibody sandwich method and AuNP amplification.

EXPERIMENTAL SECTION

Materials and Reagents. Bovine serum albumin (BSA, ≥96%), N-hydroxysuccinimide (NHS), and 1-ethyl-3-(3-dimethylaminopropyl) carbodiimide hydrochloride (EDC) were purchased from Sigma-Aldrich (St. Louis, MO). Anti-CD63 antibody and biotinylated anti-EpCAM antibody were purchased from Abcam (Cambridge, U.K.). The human liver cancer HepG2 cell line was obtained from American Type Culture Collection. Mercapto acetic acid was purchased from Aladdin Industrial Corporation (Shanghai, China). All other chemicals were of analytical grade. Ultrapure water used in all runs was obtained from a Millipore water purification system (18.2 MΩ/cm resistivity, Milli-Q Direct 8).

Cell Culture. HepG2 cell was cultured in the Dulbecco's modified Eagle's medium (DMEM, Cellgro). The culture medium contained about 1% 100 U/mL penicillin, 1% 100 μg/mL streptomycin, and 10% fetal bovine serum. Cells were cultured at 37°C with a 5% CO_2 humidified incubator.

Purification of Exosomes. The exosomes were collected and purified from the conditional medium after cells were cultured in the exosome-depleted medium for 48 h. Then, a standardized kit (SBI, Australia) was used to distinguish the exosomes from the conditional medium, as described in previous works by our research group.[40,41] First, the medium was centrifuged at 4 °C and 300*g* for 10 min to remove the excess residual cells. To remove the cell debris and apoptotic blebs, 20 min centrifugation at 2000*g* was then performed.

https://dx.doi.org/10.1021/acssensors.9b01869
ACS Sens. 2020, 5, 362−369

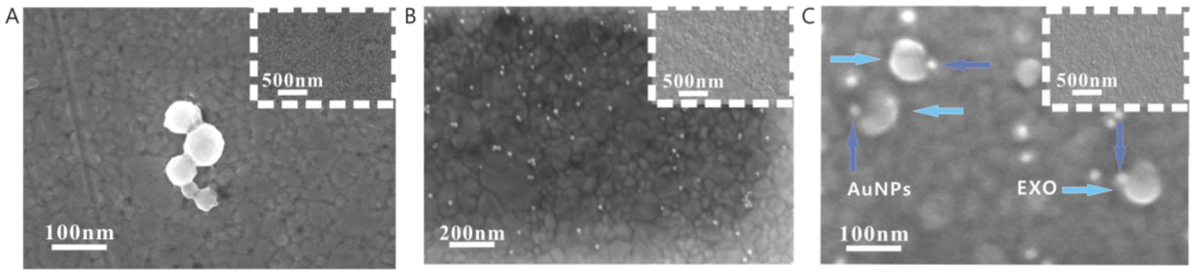

Figure 2. SEM characterization of the SAW chips. (A) Exosomes captured on the chip while their typical structure could be seen. Inset: a blank control. (B) Conjugation of AuNP onto the chip via biotin−avidin recognition. Inset: a blank control in the absence of exosomes. (C) Visualization of both exosomes and AuNP on the chip surface. Inset: a blank control in the absence of exosomes.

A 0.22 μm pore filter (Millipore, China) was then used to filter the supernatant. After that, the filtrate was further centrifuged for 30 min at 10 000*g* to remove the cell vesicles and biomacromolecules. The supernatant was again centrifuged several times at 4000*g* for 30 min to collect exosomes. The kit was then used to precipitate exosomes, and the residual sediment was resuspended in sterile buffer (Hyclone, Utah) and stored at −80 °C for the next step.

Preparation of the Sensor Chip. The SAW chip was purchased from SAW Instruments GmbH (Bonn, Germany). The chip is made up of five identical sensing channels, and each of them has a working area of 4 × 1.7 mm^2. The main components of the chip are a spacer, a silicon dioxide guiding layer, the Interdigital transducers (IDTS), and a gold-plated layer. The optical image of the chip layout is given in Figure S1. The modification of the chip and the subsequent detection were conducted in our laboratory. First, the SAW chips were immersed in a piranha solution (H_2SO_4/H_2O_2 = 3:1) for at least 1 min. Then, the chips were further sonicated in ultrapure water and ethanol each for 5 min to remove the residual organic matter from the surface. The self-assembly via the Au−S bond was completed by dropping 15 μL of 10 mM mercapto acetic acid (COOH-SAM) on detection channels of the chips, and the chips were placed for 12 h in the dark at room temperature. The anti-CD63 antibody (20 μg/mL) was immobilized on the chip by carboxyl-group activation with a mixture of 200 mM EDC and 50 mM NHS. The chips underwent washing with PBS 3 times. After that, the detection channels were treated with the BSA solution as a blocking agent, followed by washing with PBS 3 times. Then, 15 μL of NTA-calibrated exosome solution was incubated on the top of the detection channels at 37 °C for 40 min. Unbound exosomes were removed by washing the chips with PBS 3 times. Then, 15 μL of 20 μg/mL biotin-conjugated EpCAM antibodies was introduced and incubated for 45 min, followed by washing the chips with PBS 3 times.

Surface Acoustic Wave Detection. A sam5 detection instrument (SAW Instruments GmbH, Bonn, Germany) was used for the quantitative detection of exosomes. The instrument provides phase signal and amplitude signal outputs. In the present study, we always chose the phase signal as the detection signal. The two-frequency mode was chosen to confirm this measurement, resulting in a frequency difference of 0.363 (phase difference ~180^0) to optimize the frequency value. After the detection chip was loaded onto the machine and a stable baseline was obtained, 80 μL of streptavidin-modified AuNP was injected during 600 s total contact time at a flow rate of 40 μL/min. The phase shift signal was then recorded and exported to the data processing software after each injection.

RESULTS AND DISCUSSION

Exosomes Characterization. To obtain the hepatic carcinoma-specific exosomes, exosomes were separated and extracted from the culture medium of HepG2 cell lines by the above-mentioned method. The obtained exosomes were characterized by TEM, NTA, and western blotting, respectively. The specific operation of the above-mentioned experiments was the same as the previous article of our research group. The specific operation steps can be seen in the Supporting Information. As seen in the TEM image (Figure S2A), a prototypical double membrane morphology was observed for a majority of exosomes and the diameter of exosomes was about 150 nm. NTA measurement revealed that the size distribution was within the range of 50−200 nm, the concentration was about 4.7 × 10^{10} particles/mL (Figure S2B), and the average size of the exosomes was about 130 nm (Figure S2C). The results of western blotting also clearly showed the expression of CD63 and EpCAM in exosomes (Figure S2D). These characterization results indicate that a large number of exosomes with narrow and uniform size can be obtained according to our strategy. Besides, as a general method, exosomes from other cell lines and clinical samples were tested by western blotting. As can be seen in Figure S3, both CD63 and EpCAM were highly expressed in exosomes from MCF-7 and PANC-1 cell lines and lung patient samples, demonstrating the broad applicability of the sensing platform.

Feasibility Study. As discussed in the above-mentioned methods, exosomes were bound to the anti-CD63-immobilized SAW chip and AuNP was then conjugated onto the chip for the signal amplification. In this work, SEM was used to confirm the capture of exosomes and the attachment of AuNP onto the SAW chips. As observed in Figure 2A, it was clear that exosomes with their characteristic bilayer membrane structure were present on the channels of the sensors. Meanwhile, exosomes were invisible on the chip in a blank control experiment, while exosomes were not added to the chip (inset). This means that exosomes have been anchored onto the SAW chip through binding between CD63 of exosomes and the immobilized anti-CD63. In Figure 2B, the AuNP with uniform sizes was clearly seen after the biotin-conjugated antibodies and streptavidin-modified AuNP were added onto the chip. For comparison, when only the antibodies and AuNP were added on the chip in the absence of exosomes, the AuNP on the chip was barely visible. To verify that these small particles shown in Figure 2B are indeed AuNP, an EDS experiment was conducted, and the EDS characterization results are shown in Figure S4. The EDS results show that there are a large number of AuNP on the chip surface, demonstrating that these small particles shown in Figure 2B are indeed AuNP and other substances like carbon, oxygen, silicon, etc. may come from the substance materials. Meanwhile, because the chip was not dehydrated or any protective measure against biological specimens was not taken, exosomes were not visible in Figure 2B.[17] To visualize the coappearance of exosomes and AuNP, one more SEM image was obtained after the surface of the chip was treated with dehydration and metal sputtering. The SEM image shown in Figure 2C reveals

https://dx.doi.org/10.1021/acssensors.9b01869
ACS Sens. 2020, 5, 362−369

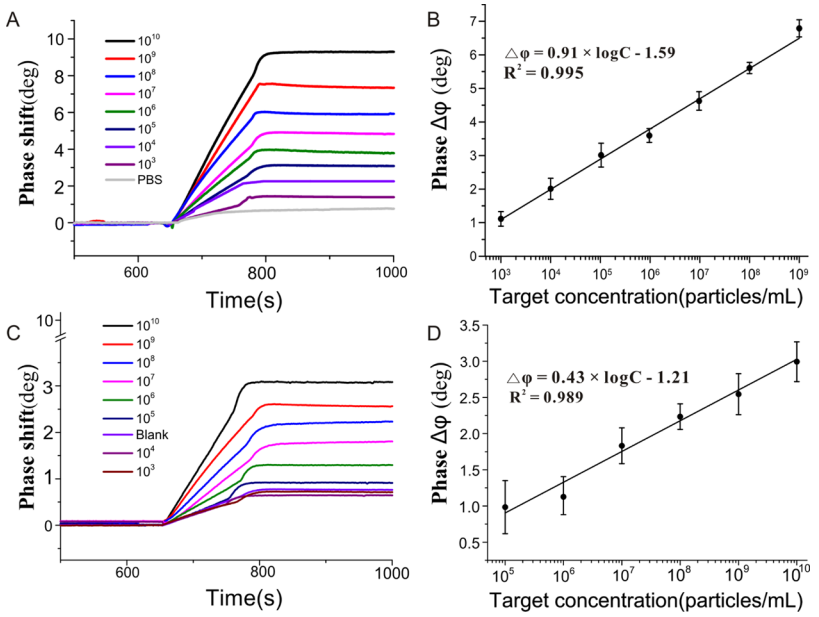

Figure 3. (A) Phase shift of the SAW sensor in response to different concentrations of exosomes (from 10^3 to 10^{10} particles/mL) with signal amplification using AuNP. (B) Calibration curve of linear relationship corresponding to (A); the exosome concentration ranged from 10^3 to 10^9 particles/mL. Error bars represent standard deviations of measurements (n = 5). (C) Phase shift of the SAW sensor in response to different concentrations of exosomes (from 10^3 to 10^{10} particles/mL) when the exosomes are directly dropped onto the CD63-modified chip. (D) Calibration curve of the linear relationship between the change of phase signal ($\triangle\varphi$) and the logarithm of exosome concentration ranging from 10^5 to 10^{10} particles/mL. Error bars represent standard deviations of measurements (n = 5).

that both exosomes and AuNP can be visible. The results demonstrate that the successful capture of exosomes and the conjugation of AuNP onto the SAW chip are realized, as anticipated.

Optimization of Detection Conditions. Multiple parameters, such as the antibody concentration, incubation time, and incubation temperature, influence the experimental results. Therefore, the experimental conditions were optimized. First, the concentrations of capture antibodies (anti-CD63) were optimized by varying antibody concentrations. As seen in Figure S5A, with increasing antibody concentrations ranging from 1 to 50 μg/mL, the SAW signal also increased and gradually stabilized when the antibody concentrations reached 20 μg/mL. The increased exosomes could be captured on the sensor chip as the concentrations of the antibody increased. However, excess numbers of antibodies could cause steric hindrance on the sensor surface, making it difficult for more exosomes to be captured. In the meantime, the various concentrations of biotin-conjugated EpCAM antibodies were investigated. As seen in Figure S5B, when the antibody concentrations were within a certain range of 1−50 μg/mL, the sensor signal increased with increasing antibody concentrations. This is because more AuNPs can be attached onto the chips as the concentrations of the antibody increases. Similar to the above-mentioned discussion, the application of excess biotin-conjugated EpCAM antibodies leads to negligible signal enhancement. As a result, the signal of the instrument is no longer increased or even reduced. Therefore, in this work, we chose 20 μg/mL as the optimal CD63 concentration and 20 μg/mL as the optimal biotin-modified antibody concentration. In addition to the concentrations of the capture antibody and biotin-modified secondary antibody, the effect of incubation time and incubation temperature during the experiment was also investigated. It can be seen from Figure S5C that the phase shift change caused by exosomes could reach the maximum value at about 7° when the temperature was maintained at 37 °C. Maintaining this temperature during the experiment allowed the exosomes to retain their original morphological structure, thereby maximizing the detection signal. Similarly, as seen in Figure S5D, when we set the incubation time of the exosomes to 40 min, the phase shift change value reached the maximum. We speculate that a short incubation time might lead to low efficiency of binding between antibodies and exosomes and a long incubation time might lead to exosome rupture. Therefore, 37 °C and 40 min were chosen as the optimal conditions.

Sensitivity of Exosome Detection. Next, the sensitivity of the sensor was investigated by applying a series of different concentrations of exosomes to the anti-CD63-modified SAW sensor under the optimal experimental conditions. As observed in Figure 3A, with the injection of AuNP, the phase signals gradually increased and remained stable after the injection. Moreover, the phase signals increased with the increasing concentration of exosomes. When exosome concentrations were increased from 0 to 4.7×10^{10} particles/mL, the phase shift signals also rose dramatically. In the presence of 4.7×10^{10} particles/mL exosomes, the amplified SAW phase shift could reach up to ~10°. However, in the case where exosomes were absent, the phase shift (~1°) was found to be negligible. This phenomenon indicates that AuNP can be successfully attached onto the chip surface in the presence of exosomes via the biotin−avidin affinity, resulting in an increase in phase shift changes. It was also observed that the phase shift change of the acoustic wave ($\triangle\varphi$, the difference value between the exosome-responsive signal change and that without exosome) was logarithmically related to the target concentrations spanning from 10^3 to 10^9 particles/mL (Figure 3B). The phase shift change ($\triangle\varphi$) had a linear relationship with the logarithmic value of target exosome concentrations (C), and the regression equation is $\triangle\varphi = 0.91 \times \log C - 1.59$, R^2 =

https://dx.doi.org/10.1021/acssensors.9b01869
ACS Sens. 2020, 5, 362−369

0.995; the detection limit was estimated to be 1.1×10^3 particle/mL by equation $S = 3\sigma$ (S is the signal difference value of 1.1×10^3 particles/mL and blank, and σ is the standard deviation of the baseline). To better exhibit the advantages of the SAW sensor for exosome detection, the sensor performance has been compared with other platforms, and the comparison is presented in Table 1. The sensitivity of this method is superior to that of the conventional fluorescent and other commonly used approaches.

Table 1. Comparison of Currently Available Methods for the Detection of Exosomes

method	LOD (particles/mL)	references
RGO field-effect transistor biosensor	3.3×10^4	41
paper-based aptasensor	1.1×10^6	43
UV−vis absorbance measurement	2.76×10^6	44
electrochemical detection method	2.09×10^4	45
surface-enhanced Raman scattering	1.2×10^6	46
fluorescence measurement	5×10^4	47
electrochemical sandwich immunosensor	2×10^5	48
AuNP-amplified SAW immunosensor	1.1×10^3	this work

To verify that the signal amplification is caused by the application of AuNP, the sensor performance was compared with the direct detection of exosomes in the absence of AuNP. After the SAW chip was modified with anti-CD63 and the chip was loaded onto the machine, 15 μL of exosomes was injected during 600 s total contact time at a 40 μL/min flow rate. The phase signal was then recorded and exported to the data processing software after each injection. As shown in Figure 3C, the change of the phase signals also increased along with the increase of exosomes concentrations from 10^5 to 10^{10} particles/mL. However, the phase signal amplified by AuNP was much larger than that without AuNP in the same concentration range (10^5−10^{10} particles/mL). The specific linear relationship between them can be seen in Figure 3D with a regression equation ($\triangle\varphi = 0.43 \times \log C - 1.21$, $R^2 = 0.989$), and the detection limit could be estimated as 8.4×10^4 particles/mL by the above formula. As seen in Figure 3A,C, the signal of negative controls is negligible. The standard deviations of the negative controls were calculated to be 0.39 and 0.31, respectively. It is clear that the detection limit obtained by AuNP amplification is appropriate 2 orders of magnitude lower than that obtained by the direct detection. Although the binding of exosomes on the SAW chips can increase the response signal, the introduction of AuNP can significantly amplify the instrument's signal, thereby greatly increasing the sensitivity of this detection method.

Selectivity of the SAW Sensor. The selectivity of this method was also investigated by changing the various types of capture proteins and the detection substances. First, to test the discriminating capacity of this bioassay, several human antibodies, like CD86, BNP, LCN-2, and BSA, as capture proteins, respectively, were selected to investigate the change of the instrument signal shift. As shown in Figure 4A, only in the presence of CD63, the instrument's signal value reached the maximum at 7.312°. In comparison, a negligible phase shift was observed after exosomes were applied to the nonspecific antibody (CD86, BNP, LCN-2, BSA)-functionalized SAW biosensor. The phase shifts were found to be 3.06, 2.11, 2.57, and 1.37°, respectively, which is slightly higher than that of the blank when PBS was used as a capture substance (<1.0°), approximately 1/3 of that of the specific antibody. These results demonstrate that theCD63 antibody can specifically bind to the antigen on the surface of exosomes and significantly increase the signal of the instrument.

Due to the significance of the sensor selectivity, especially in clinical applications, we also used exosomes, microvesicles (MVs), and several tumor markers like α fetoprotein (AFP), prostate-specific antigen (PSA), and carcinoembryonic antigen (CEA) as detection substances to investigate the discrimination capability of this assay. For the isolation of MVs, a standard ultracentrifugation method with slight modifications was used to distinguish MVs from the conditional medium, as described in the previous work by our research group.[42] The obtained MVs were characterized by TEM. As can be seen in Figure S6, a prototypical double-membrane morphology was observed and the diameter of MV was about 800 nm, indicating the successful extraction of MVs. The anti-CD63-functionalized SAW biosensor was used to detect 10 μg/mL nonspecific proteins AFP, PSA, and CEA; 10^6 particles/mL exosomes; 10^9 particles/mL exosomes; MVs (10^8 particles/mL); and a mixture (exosome + MVs), respectively. From the results in Figure 4B, the phase shift rose significantly only in the presence of exosomes. An obvious difference between the noise and 10^6 particles/mL exosomes was obtained, indicating that the lower detection limit can be achieved. In a mixed

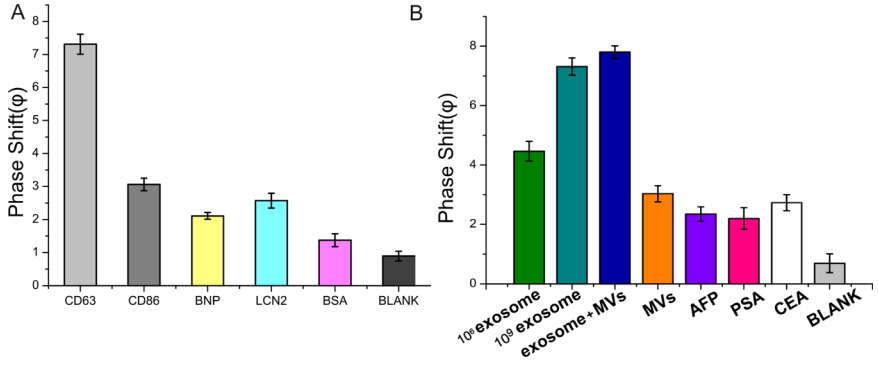

Figure 4. Selectivity of the SAW sensor. (A) Sensor response comparison among anti-CD63 and diverse capture proteins, which were immobilized on the SAW chip. Error bars represent standard deviations of measurements (n = 5). (B) Response of the CD63-modified SAW chip to various detection substances, where the concentration of capture CD63 antibody was 20 μg/mL. Error bars represent standard deviations of measurements (n = 5).

https://dx.doi.org/10.1021/acssensors.9b01869
ACS Sens. 2020, 5, 362−369

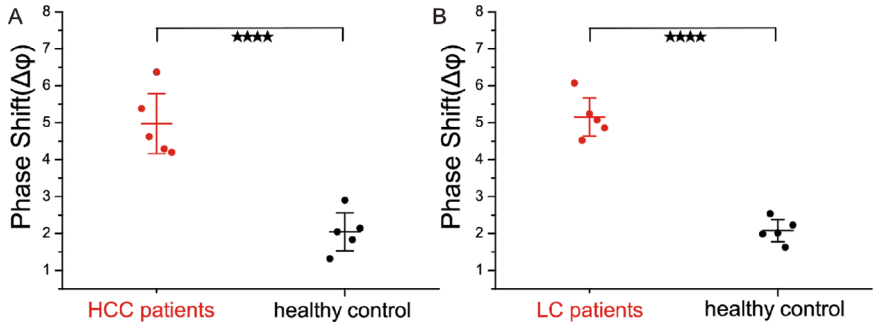

Figure 5. Response of the SAW sensor to exosomes obtained from clinical plasma samples of cancer patients and healthy people. (A) Comparison of expressions of different exosomes between healthy controls and HCC (hepatocellular carcinoma cancer) patients. (B) Comparison of expression of different exosomes between healthy controls and LC (lung cancer) patients. Compared with healthy controls, patients' sera show a significantly elevated level of exosomes ($p < 0.0001$). All measurements were carried out in triplicate, and the data are shown as mean ± s.d. a.u., arbitrary unit.

solution containing both exosomes and MVs as described above, the phase shift caused by the mixture solution was 7.79°, which is consistent with the previous reports.[40,41] However, the nonspecific MVs only caused the phase shift of 3.04°. Similarly, other nonspecific tumor markers including AFP, PSA, and CEA could only result in phase shifts of 2.52, 2.32, and 2.81°, respectively. The nonspecific signals from MVs, AFP, PSA, and CEA seemed to be a bit larger than that of the blank. It is probably caused by nonspecific binding of these substances on the chip surface. The results indicate that the SAW biosensors possess great selectivity and have a wide range of applications in the complex environment.

Detection of Clinical Samples. To evaluate the performance of this bioassay in clinical applications, the SAW sensor's capability of detecting target exosomes from blood samples of cancer patients and healthy people was examined. Clinical samples were obtained by collecting blood samples from a total of 20 volunteers. The basic information about patients and healthy controls is presented in Table S1. The 10 samples in the control group were all obtained from healthy volunteers during a routine examination at the Wuhan Hospital of Integrated Traditional Chinese and Western Medicine (Wuhan, China). Five cases of liver cancer patients and five cases of lung cancer patients were obtained from the Central Hospital of Wuhan (Wuhan, China). The collected frozen plasma was first centrifuged to remove the cell debris, and then, thrombin was added to remove fibrin. For the isolation of plasma exosomes, a standard kit (SBI, Australia) was used to distinguish exosomes from the clinical samples, as described in previous works by our research group.[40,41] After exosomes were obtained from the blood samples and applied to the anti-CD63-modified SAW chips, the response signals obtained in healthy volunteer samples were compared with the corresponding signals obtained from the cancer patients. Figure 5A compares the expression levels of exosomes between hepatocellular carcinoma cancer patients and healthy individuals, while Figure 5B shows the difference in exosome expression levels between lung cancer patients and healthy individuals. As clearly shown in Figure 5A,B, the SAW sensor incubated with patients' exosomes achieved a superior variation of phase shift. However, a negligible phase shift was obtained when the chip was incubated with healthy volunteers' exosomes. The distinct profiles indicate a significant difference in the level of exosome expression between healthy volunteers and patients with different types of cancer. The result corroborates the significant improvement of exosomes expressed in cancer patients as compared to that in healthy volunteers ($p < 0.05$). However, due to the extensive expression of CD63 in the exosomes of different cancers, the biosensors cannot distinguish patients from patients with different types of cancers. Despite this, the results shown in Figure 5 reveal that this SAW detection platform is suitable for exosome detection in undiluted plasma samples. This excellent anti-interference ability mainly benefits from the special cooperative sensing interface design and the excellent pairing capacity between the capture antibody and the target antigen. Thus, the developed SAW sensor is capable of quantifying exosomes in real human biofluids. What is more, in subsequent experiments, we can also specifically detect different types of cancers by employing cancer-specific antibodies to differentiate different cancers.

CONCLUSIONS

In summary, we have built a reliable, efficient, and cost-effective method for exosome determination by combining the SAW sensor with AuNP amplification. In general, this detection approach has the following unique merits: (i) binding of streptavidin-modified AuNP to exosome-bound SAW chips through biotin-labeled EpCAM antibody yields a great mass effect above the sensing interface, thus improving the detection sensitivity; (ii) the entire measurement process takes only about half an hour, which is fast; and (iii) the biosensor should be able to reliably detect exosomes from real human blood samples via a sandwich immunoassay. These merits make our platform prospective as an impressive new technology for the quantification of exosomes in clinical practice such as individualized administration and treatment.

ASSOCIATED CONTENT

Supporting Information

The Supporting Information is available free of charge at https://pubs.acs.org/doi/10.1021/acssensors.9b01869.

Method for characterization of exosomes; optical image of the SAW chip layout; characterization of exosomes; western blot results of exosomes; EDS characterization; influence of different parameters on the SAW sensor performance; TEM image of the purified MVs; and basic information about patients and healthy controls (PDF)

https://dx.doi.org/10.1021/acssensors.9b01869
ACS Sens. 2020, 5, 362−369

AUTHOR INFORMATION

Corresponding Authors

Yulin Zhang − *School of Laboratory Medicine, Hubei University of Chinese Medicine, Wuhan 430065, P. R. China*

Qunfeng Yao − *School of Laboratory Medicine, Hubei University of Chinese Medicine, Wuhan 430065, P. R. China*

Guo-Jun Zhang − *School of Laboratory Medicine, Hubei University of Chinese Medicine, Wuhan 430065, P. R. China;* orcid.org/0000-0001-9096-9226; Phone: +86-27-68890259; Email: zhanggj@hbtcm.edu.cn

Authors

Chenyun Wang − *School of Laboratory Medicine, Hubei University of Chinese Medicine, Wuhan 430065, P. R. China*

Cancan Wang − *School of Laboratory Medicine, Hubei University of Chinese Medicine, Wuhan 430065, P. R. China*

Dan Jin − *School of Laboratory Medicine, Hubei University of Chinese Medicine, Wuhan 430065, P. R. China*

Yi Yu − *School of Laboratory Medicine, Hubei University of Chinese Medicine, Wuhan 430065, P. R. China*

Fan Yang − *School of Laboratory Medicine, Hubei University of Chinese Medicine, Wuhan 430065, P. R. China;* orcid.org/0000-0002-8490-4183

Complete contact information is available at: https://pubs.acs.org/10.1021/acssensors.9b01869

Author Contributions

†Chenyun Wang and Cancan Wang contributed equally to this work.

Notes

The authors declare no competing financial interest.

ACKNOWLEDGMENTS

This work was supported by the National Natural Science Foundation of China (Nos. 21675041 and 21974035).

REFERENCES

(1) Siegel, R. L.; Miller, K. D.; Jemal, A. Cancer statistics, 2018. *CA: Cancer J. Clin.* **2018**, *60*, 277−300.

(2) Caesar-Johnson, S. J.; Demchok, J. A.; Felau, I.; Kasapi, M.; Ferguson, M. L.; Hutter, C. M.; Sofia, H. J.; Tarnuzzer, R.; Wang, Z.; Yang, L.; et al. The Immune Landscape of Cancer. *Immunity* **2018**, *48*, 812−830.

(3) Liu, C.; Zhao, J.; Tian, F.; Cai, L.; Zhang, W.; Feng, Q.; Chang, J.; Wan, F.; Yang, Y.; Dai, B.; et al. Low-cost thermophoretic profiling of extracellular-vesicle surface proteins for the early detection and classification of cancers. *Nat. Biomed. Eng.* **2019**, *3*, 183−193.

(4) Chen, D. S.; Mellman, I. Elements of cancer immunity and the cancer−immune set point. *Nature* **2017**, *541*, 321−330.

(5) Tian, F.; Liu, C.; Lin, L.; Chen, Q.; Sun, J. Microfluidic analysis of circulating tumor cells and tumor-derived extracellular vesicles. *TrAC, Trends Anal. Chem.* **2019**, *117*, 128−145.

(6) Melo, S. A.; Luecke, L. B.; Christoph, K.; Fernandez, A. F.; Gammon, S. T.; Judith, K.; Lebleu, V. S.; Mittendorf, E. A.; Juergen, W.; Nuh, R.; et al. Glypican-1 identifies cancer exosomes and detects early pancreatic cancer. *Nature* **2015**, *523*, 177−182.

(7) Tkach, M.; Théry, C. Communication by Extracellular Vesicles: Where We Are and Where We Need to Go. *Cell* **2016**, *164*, 1226−1232.

(8) Jpg, S.; Davidson, S. M.; Boulanger, C. M.; Iren, B. E.; Dpv, D. K.; Engel, F. B.; Giricz, Z.; Hausenloy, D. J.; Kishore, R.; Lecour, S.; et al. Extracellular vesicles in diagnostics and therapy of the ischaemic heart: Position Paper from the Working Group on Cellular Biology of the Heart of the European Society of Cardiology. *Cardiovasc. Res.* **2017**, *114*, 19−34.

(9) Soung, Y.; Ford, S.; Zhang, V.; Chung, J. Exosomes in Cancer Diagnostics. *Cancers* **2017**, *9*, No. 8.

(10) Kalluri, R. The biology and function of exosomes in cancer. *J. Clin. Invest.* **2016**, *126*, 1208−1215.

(11) Elsherbini, A.; Bieberich, E. Ceramide and Exosomes: A Novel Target in Cancer Biology and Therapy. *Adv. Cancer Res.* **2018**, *140*, 121−154.

(12) Azmi, A. S.; Bao, B.; Sarkar, F. H. Exosomes in cancer development, metastasis, and drug resistance: a comprehensive review. *Cancer Metastasis Rev.* **2013**, *32*, 623−642.

(13) Bastos, N.; Ruivo, C. F.; Silva, S.; Melo, S. A. Exosomes in Cancer: Use them or Target them? *Semin. Cell Dev. Biol.* **2017**, *78*, 13−21.

(14) Carretero-González, A.; Otero, I.; Carril-Ajuria, L.; Velasco, G. D.; Manso, L. Exosomes: Definition, Role in Tumor Development and Clinical Implications. *Cancer Microenviron.* **2018**, *11*, 13−21.

(15) Iero, M.; Valenti, R.; Huber, V.; Filipazzi, P.; Parmiani, G.; Fais, S.; Rivoltini, L. Tumour-released exosomes and their implications in cancer immunity. *Cell Death Differ.* **2008**, *15*, 80−88.

(16) Zhou, L.; Lv, T.; Zhang, Q.; Zhu, Q.; Zhan, P.; Zhu, S.; Zhang, J.; Song, Y. The biology, function and clinical implications of exosomes in lung cancer. *Cancer Lett.* **2017**, *407*, 84−92.

(17) Sokolova, V.; Ludwig, A. K.; Hornung, S.; Rotan, O.; Horn, P. A.; Epple, M.; Giebel, B. Characterisation of exosomes derived from human cells by nanoparticle tracking analysis and scanning electron microscopy. *Colloids Surf., B* **2011**, *87*, 146−150.

(18) Tatischeff, I.; Larquet, E.; Falcónpérez, J. M.; Turpin, P. Y.; Kruglik, S. G. Fast characterisation of cell-derived extracellular vesicles by nanoparticles tracking analysis, cryo-electron microscopy, and Raman tweezers microspectroscopy. *J. Extracell. Vesicles* **2012**, *1*, No. 19179.

(19) Sharma, S.; Leclaire, M.; Gimzewski, J. K. Ascent of atomic force microscopy as a nanoanalytical tool for exosomes and other extracellular vesicles. *Nanotechnology* **2018**, *29*, No. 132001.

(20) van der Pol, E.; Hoekstra, A. G.; Sturk, A.; Otto, C.; Van Leeuwen, T. G.; Nieuwland, R. Optical and non-optical methods for detection and characterization of microparticles and exosomes. *J. Thromb. Haemostasis* **2010**, *8*, 2596−2607.

(21) Kesimer, M.; Gupta, R. Physical characterization and profiling of airway epithelial derived exosomes using light scattering. *Methods* **2015**, *87*, 59−63.

(22) Soo, C. Y.; Song, Y.; Zheng, Y.; Campbell, E. C.; Riches, A. C.; Gunn-Moore, F.; Powis, S. J. Nanoparticle tracking analysis monitors microvesicle and exosome secretion from immune cells. *Immunology* **2012**, *136*, 192−197.

(23) Maas, S. L.; Broekman, M. L.; de Vrij, J. Tunable Resistive Pulse Sensing for the Characterization of Extracellular Vesicles. *Methods Mol. Biol.* **2017**, *1545*, 21−33.

(24) Anderson, W.; Lane, R.; Korbie, D.; Trau, M. Observations of Tunable Resistive Pulse Sensing for Exosome Analysis: Improving System Sensitivity and Stability. *Langmuir* **2015**, *31*, 6577−6587.

(25) Kesimer, M.; Gupta, R. Physical characterization and profiling of airway epithelial derived exosomes using light scattering. *Methods* **2015**, *87*, 59−63.

(26) Nolte-'t Hoen, E. N. M.; van der Vlist, E. J.; Aalberts, M.; Mertens, H. C. H.; Bosch, B. J.; Bartelink, W.; Mastrobattista, E.; van Gaal, E. V. B.; Stoorvogel, W.; Arkesteijn, G. J. A.; Wauben, M. H. M. Quantitative and qualitative flow cytometric analysis of nanosized cell-derived membrane vesicles. *Nanomedicine* **2012**, *8*, 712−720.

(27) Im, H.; Shao, H.; Park, Y. I.; Peterson, V. M.; Castro, C. M.; Weissleder, R.; Lee, H. Label-free detection and molecular profiling of exosomes with a nano-plasmonic sensor. *Nat. Biotechnol.* **2014**, *32*, 490−495.

(28) Tzou, H. S.; Tseng, C. I. Distributed piezoelectric sensor/actuator design for dynamic measurement/control of distributed parameter systems: A piezoelectric finite element approach. *J. Sound Vib.* **1990**, *138*, 17−34.

(29) Hwang, W.-S.; Park, H. C. Finite element modeling of piezoelectric sensors and actuators. *AIAA J.* **1993**, *31*, 930−937.

(30) Zhang, Y.; Fan, Y.; Sun, Z.; Li, Y.; Zhang, G. J. Surface acoustic wave biosensor synergizing DNA-mediated in-situ silver nanoparticle growth for highly specific and signal-amplified nucleic acid assay. *Analyst* **2017**, *142*, 3468−3476.
(31) Li, S.; Ying, W.; Yan, S.; Fan, C.; Bhethanabotla, V. R. Gold nanoparticle-based low limit of detection Love wave biosensor for carcinoembryonic antigens. *Biosens. Bioelectron.* **2017**, *95*, 48−54.
(32) Ying, J.; Tan, C. Y.; Tan, S. Y.; Wong, M. S. F.; Chen, Y. F.; Zhang, L.; Yao, K.; Gan, S. K. E.; Verma, C.; Tan, Y.-J. SAW sensor for Influenza A virus detection enabled with efficient surface functionalization. *Sens. Actuators, B* **2015**, *209*, 78−84.
(33) Chang, K.; Pi, Y.; Lu, W.; Wang, F.; Pan, F.; Li, F.; Jia, S.; Shi, J.; Deng, S.; Chen, M. Label-free and high-sensitive detection of human breast cancer cells by aptamer-based leaky surface acoustic wave biosensor array. *Biosens. Bioelectron.* **2014**, *60*, 318−324.
(34) Liu, X.; Wang, J.-Y.; Mao, X.-B.; Ning, Y.; Zhang, G.-J. Single-shot analytical assay based on graphene-oxide-modified surface acoustic wave biosensor for detection of single-nucleotide polymorphisms. *Anal. Chem.* **2015**, *87*, 9352−9359.
(35) Kanwar, S. S.; Dunlay, C. J.; Simeone, D. M.; Nagrath, S. Microfluidic device (ExoChip) for on-chip isolation, quantification and characterization of circulating exosomes. *Lab Chip* **2014**, *14*, 1891−1900.
(36) Zhou, Q.; Rahimian, A.; Son, K.; Shin, D. S.; Patel, T.; Revzin, A. Development of an aptasensor for electrochemical detection of exosomes. *Methods* **2016**, *97*, 88−93.
(37) Kang, Y.-T.; Kim, Y. J.; Bu, J.; Cho, Y.-H.; Han, S.-W.; Moon, B.-I. High-purity capture and release of circulating exosomes using an exosome-specific dual-patterned immunofiltration (ExoDIF) device. *Nanoscale* **2017**, *9*, 13495−13505.
(38) Yao, X.; Li, X.; Toledo, F.; Zurita-Lopez, C.; Gutova, M.; Momand, J.; Zhou, F. Sub-attomole oligonucleotide and p53 cDNA determinations via a high-resolution surface plasmon resonance combined with oligonucleotide-capped gold nanoparticle signal amplification. *Anal. Biochem.* **2006**, *354*, 220−228.
(39) Wang, Q.; Zou, L.; Yang, X.; Liu, X.; Nie, W.; Zheng, Y.; Cheng, Q.; Wang, K. Direct quantification of cancerous exosomes via surface plasmon resonance with dual gold nanoparticle-assisted signal amplification. *Biosens. Bioelectron.* **2019**, *135*, 129−136.
(40) Jin, D.; Yang, F.; Zhang, Y. L.; Liu, L.; Zhou, Y.; Wang, F.; Zhang, G.-J. ExoAPP: Exosome-Oriented, Aptamer Nanoprobe-Enabled Surface Proteins Profiling and Detection. *Anal. Chem.* **2018**, *90*, 14402−14411.
(41) Yu, Y.; Li, Y.-T.; Jin, D.; Yang, F.; Wu, D.; Xiao, M.; Zhang, H.; Zhang, Z.; Zhang, G.-J. Electrical and Label-Free Quantification of Exosomes with Reduced Graphene Oxide Field Effect Transistor Biosensor. *Anal. Chem.* **2019**, *91*, 10679−10686.
(42) Wu, D.; Zhang, H.; Jin, D.; Yu, Y.; Pang, D.-W.; Xiao, M.-M.; Zhang, Z.-L.; Zhang, Z.-Y.; Zhang, G.-J. Microvesicle detection by a reduced graphene oxide field-effect transistor biosensor based on a membrane biotinylation strategy. *Analyst* **2019**, *144*, 6055−6063.
(43) Chen, X.; Lan, J.; Liu, Y.; Li, L.; Yan, L.; Xia, Y.; Wu, F.; Li, C.; Li, S.; Chen, J. A paper-supported aptasensor based on upconversion luminescence resonance energy transfer for the accessible determination of exosomes. *Biosens. Bioelectron.* **2017**, *102*, 582−588.
(44) Vaidyanathan, R.; Naghibosadat, M.; Rauf, S.; Korbie, D.; Carrascosa, L. G.; Shiddiky, M. J.; Trau, M. Detecting exosomes specifically: a multiplexed device based on alternating current electrohydrodynamic induced nanoshearing. *Anal. Chem.* **2014**, *86*, 11125−11132.
(45) Wang, S.; Zhang, L.; Wan, S.; Cansiz, S.; Cui, C.; Liu, Y.; Cai, R.; Hong, C.; Teng, I. T.; Shi, M.; et al. Aptasensor with Expanded Nucleotide Using DNA Nanotetrahedra for Electrochemical Detection of Cancerous Exosomes. *ACS Nano* **2017**, *11*, 3943−3949.
(46) Zong, S.; Wang, L.; Chen, C.; Lu, J.; Zhu, D.; Zhang, Y.; Wang, Z.; Cui, Y. Facile detection of tumor-derived exosomes using magnetic nanobeads and SERS nanoprobes. *Anal. Methods* **2016**, *8*, 5001−5008.
(47) Zhang, P.; He, M.; Zeng, Y. Ultrasensitive microfluidic analysis of circulating exosomes using a nanostructured graphene oxide/polydopamine coating. *Lab Chip* **2016**, *16*, 3033−3042.
(48) Doldán, X.; Fagúndez, P.; Cayota, A.; Laíz, J.; Tosar, J. P. Electrochemical Sandwich Immunosensor for Determination of Exosomes Based on Surface Marker-Mediated Signal Amplification. *Anal. Chem.* **2016**, *88*, 10466−10473.

https://dx.doi.org/10.1021/acssensors.9b01869
ACS Sens. 2020, 5, 362−369